Interdomain zinc site on human albumin

Alan J. Stewart*, Claudia A. Blindauer*, Stephen Berezenko†, Darrell Sleep†, and Peter J. Sadler*‡

*School of Chemistry, University of Edinburgh, West Mains Road, Edinburgh EH9 3JJ, United Kingdom; and †Delta Biotechnology Ltd., Castle Court, Castle Boulevard, Nottingham NG7 1FD, United Kingdom

Edited by Jack Halpern, University of Chicago, Chicago, IL, and approved December 20, 2002 (received for review October 30, 2002)

Albumin is the major transport protein in blood for Zn^{2+}, a metal ion required for physiological processes and recruited by various drugs and toxins. However, the Zn^{2+}-binding site(s) on albumin is ill-defined. We have analyzed the 18 x-ray crystal structures of human albumin in the PDB and identified a potential five-coordinate Zn site at the interface of domains I and II consisting of N ligands from His-67 and His-247 and O ligands from Asn-99, Asp-249, and H_2O, which are the same amino acid ligands as those in the zinc enzymes calcineurin, endonucleotidase, and purple acid phosphatase. The site is preformed in unliganded apo-albumin and highly conserved in mammalian albumins. We have used ^{111}Cd NMR as a probe for Zn^{2+} binding to recombinant human albumin. We show that His-67 → Ala (His67Ala) mutation strongly perturbs Cd^{2+} binding, whereas the mutations Cys34Ala, or His39Leu and Tyr84Phe (residues which may H-bond to Cys-34) have no effect. Weak Cl^- binding to the fifth coordination site of Cd^{2+} was demonstrated. Cd^{2+} binding was dramatically affected by high fatty acid loading of albumin. Analysis of the x-ray structures suggests that fatty acid binding to site 2 triggers a spring-lock mechanism, which disengages the upper (His-67/Asn-99) and lower (His-247/Asp-249) halves of the metal site. These findings provide a possible mechanism whereby fatty acids (and perhaps other small molecules) could influence the transport and delivery of zinc in blood.

Zinc is an essential element in the body, being critical for the development and function of all cells, for the immune system, and for transmission of genetic information. It has catalytic or structural roles in a wide range of proteins (1), including anthrax lethal factor (2). Recruitment of Zn^{2+} activates some bacterial enterotoxins (3) and is being used as a drug design strategy for enhancing the potency of organic serine protease inhibitors (4).

The concentration of Zn^{2+} in blood plasma is ≈19 μM, most of which is bound to albumin [affinity constant for human serum albumin (HSA) log $K_d = -7.53$; ref. 5], but the specific binding sites for Zn^{2+} on albumin have not yet been located. Albumin modulates zinc uptake by endothelial cells (6), and receptor-mediated vesicular cotransport across the endothelium has been demonstrated for zinc-albumin complexes *in vitro* (7). Albumin also facilitates uptake of Zn^{2+} by erythrocytes (8), where it binds to glutathione (9) and hemoglobin (log $K_d = -7.7$; ref. 10) and increases its oxygen affinity (11).

Human albumin (66.5 kDa), a single chain of 585 amino acids, is the most abundant protein in blood plasma, typically present at concentrations of ≈0.6 mM (12). It consists of three structurally homologous, largely helical (67%) domains I, II, and III (Fig. 1*A*; refs. 13–16). Each domain consists of two subdomains, A and B. Like other mammalian albumins, human albumin contains 17 disulfide bridges and a free thiol at Cys-34 (12).

It is clear from previous publications (17–19) that serum albumin has a variety of metal sites with different specificities, although the reported data are somewhat ambiguous. The best characterized metal sites on albumin are those for Cu^{2+} and Ni^{2+}, which bind strongly to a square-planar site of four nitrogen ligands from Asp-1-Ala-2-His-3 at the N terminus (20–22), and for Au^+ (from antiarthritic drugs), which binds to the thiolate sulfur at Cys-34 (23). CD studies suggest that the major Zn^{2+} site is also a secondary (weaker) binding site for Cu^{2+} and Ni^{2+} (17). Early ^{113}Cd NMR experiments on BSA demonstrated the existence of two Cd^{2+}-binding sites (18), A and B. Competition experiments on bovine and HSAs (18, 19, 24) have shown that site A binds Zn^{2+} more strongly than Cd^{2+}. NMR peaks A (130 ppm in phosphate buffer) and B (24 ppm) were also observed when ^{113}Cd was added to intact human blood serum, although peak A was shifted downfield by 15 ppm (24). The variability of the line width of peak A from different batches of albumin (especially defatted) was also noted (24).

Albumin isolated from blood serum or plasma is usually heterogeneous. This heterogeneity is caused by factors such as the variable extent of oxidation of the thiol at Cys-34 (e.g., as a disulfide) and variations in the number and types of bound fatty acids. In the present work, we have attempted to avoid this problem by carrying out experiments with recombinant human albumin (rHA), which has a high thiol content (> 0.7 SH per mol, Cys-34) and is homogeneous in bound fatty acid (octanoate).

On the basis of a detailed comparison of the 18 x-ray crystal structures of human albumin available in the PDB, together with competitive Zn^{2+}/Cd^{2+}-binding studies using ^{111}Cd NMR, mutagenesis and molecular modeling studies, we propose a new model for the high-affinity Zn^{2+} site and a mechanism for fatty-acid-induced switching of its ligand environment. Our findings will allow exploration of novel approaches for the control of zinc transport and delivery of potential importance in drug design and therapy.

Materials and Methods

Mutagenesis, Protein Expression, and Purification. Oligonucleotide-directed mutagenesis was used to prepare cDNAs encoding the mutated albumins. Mutagenesis was typically performed by using the QuikChange Site-Directed Mutagenesis kit (Stratagene). A clone containing the desired mutation was identified by nucleotide sequence analysis across the mutation site by dideoxy chain termination sequencing. The mutated cDNA was inserted in a pAYE316-based yeast expression plasmid (25), and *Saccharomyces cerevisae* DXY1 (26) was transformed to leucine prototrophy by electroporation. Recombinant albumin was expressed in *S. cerevisiae* DXY1 cells and purified by cation-exchange chromatography on SP-Sepharose (Amersham Pharmacia; final elution 85 mM sodium acetate containing 5 mM octanoic acid, pH 5.5), anion-exchange chromatography on DEAE (Amersham Pharmacia; elution with 110 mM borate, pH 9.4) and by affinity chromatography on Delta Blue Agarose (ProMetic Biosciences, Cambridge, U.K.; elution with 50 mM phosphate buffer containing 2 M NaCl, pH 6.9). Purity of the proteins by SDS/PAGE was >99%, and electrospray ionization-MS of native and mutant proteins gave peaks within ±4 amu of the calculated masses. Where studied (H39L, Y84F, H67A), the CD spectra of the mutants were similar to the native protein showing that

This paper was submitted directly (Track II) to the PNAS office.

Abbreviations: rHA, recombinant human albumin; HSA, human serum albumin.

‡To whom correspondence should be addressed. E-mail: p.j.sadler@ed.ac.uk.

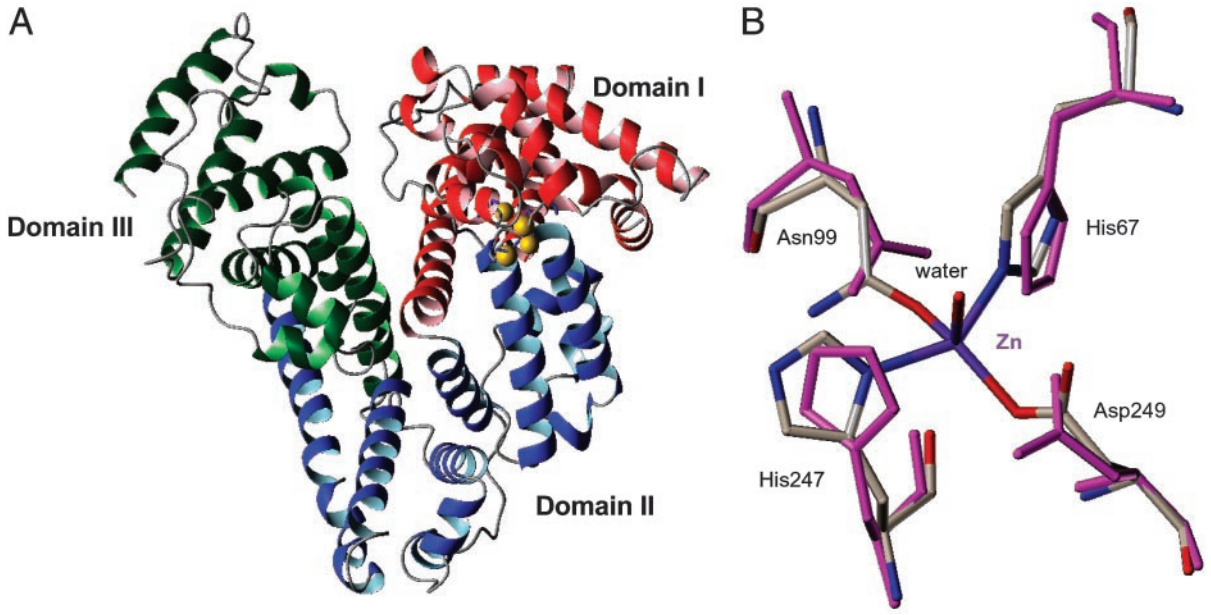

Fig. 1. Proposed Zn^{2+}-binding site in HSA. (*A*) Domain structure of albumin (PDB ID code 1AO6): domain I is colored red (residues 1–181), domain II is blue (residues 188–373), domain III is green (residues 380–571), and connecting helices are the same color as the preceding domain. The ligand atoms for Zn^{2+} (Nϵ of His-67, Nδ of His-247, amide oxygen of Asn-99, and carboxyl oxygen of Asp-249) are highlighted in yellow. (*B*) Overlay of the Zn^{2+}-binding site in the x-ray structure of unliganded rHA (PDB ID code 1AO6, magenta) and in an energy-minimized model with Zn^{2+} bound (CPK coloring). The orientation is similar to that in *A*.

the mutations did not cause any significant changes in secondary structure (Fig. 5, which is published as supporting information on the PNAS web site, www.pnas.org).

Aliquots of the mutant proteins (800 mg in 20 ml of 50 mM phosphate buffer/2 M NaCl) and native rHA (3.8 mM, 145 mM NaCl, containing 15 mg·l^{-1} Tween-80 and 40 mM octanoic acid) were routinely dialyzed twice in 100 mM ammonium carbonate (277 K, 5 liters, 24 h) before use in metal-binding experiments. Dialysis reduced the amount of octanoate bound to rHA (from $\approx$8 to $<$4 mol per mol of protein). Chicken albumin (Cohn fraction V, 99% pure) was purchased from NBS Biologicals (Huntingdon, U.K.) and was dialyzed against 100 mM ammonium carbonate and lyophilized before use.

Optical Spectroscopy. CD spectra were recorded on a JASCO J-600 spectropolarimeter by using $\approx$23 μM solutions of rHA in 0.2 M potassium phosphate, pH 7.4. The SELCON procedure (27) was used for secondary structure analysis.

^{111}Cd NMR Spectroscopy. ^{111}Cd and ^{113}Cd are both spin-1/2 nuclei with similar magnetic properties and are useful probes for Zn^{2+}-binding sites in proteins. Their chemical shifts are diagnostic of the number and types of bound ligands (28) and, with enrichment to $>$90%, can readily be detected at millimolar concentrations. ^{111}Cd-NMR studies were carried out by using 1.5 mM solutions of albumin in 50 mM Tris, pH 7.1/50 mM NaCl/10% D_2O/90% H_2O with 2 mol equivalent of $^{111}CdCl_2$. For metal titrations, aliquots of concentrated aqueous solutions of $^{111}CdCl_2$, $^{111}CdClO_4$ [generated by dissolving ^{111}CdO, 95.11% isotopic purity (Oak Ridge National Laboratory, Oak Ridge, TN) in 1 M HCl or $HClO_4$, respectively], or $ZnCl_2$ were added. The pH was checked and adjusted (if required) after each addition. For the chloride titration, aliquots of aqueous solutions of 1–4 M NaCl were added to 1.5 mM rHA in 100 mM potassium phosphate buffer, pH 7.1/10% D_2O/90% H_2O, to which 2 mol equivalent of $^{111}Cd(ClO_4)_2$ had been added.

1D ^{111}Cd-{^{1}H} NMR spectra (106.04 MHz, Bruker DMX500; Bruker, Coventry, U.K.) were acquired by using a 10-mm BBO (direct observe) probe head, with 0.1 M $Cd(ClO_4)_2$ (0 ppm) as an external standard. Proton decoupling was achieved by inverse-gated composite pulse decoupling using GARP. Spectra were acquired over a sweep width of 30 kHz (280 ppm) into 6,144 complex data points, with a ^{111}Cd pulse width of 17.5 μs (90°), 36,864 transients, acquisition time of 0.10 s, and a recycle delay of 0.3 s. Before Fourier transformation, data were zero-filled to 16,384 data points and apodized by exponential multiplication (120 Hz line-broadening).

Molecular Modeling. The initial model of Zn-albumin was based on a published crystal structure of unliganded (apo)-albumin (PDB ID code 1AO6) by using WEBLAB VIEWERPRO V.4.0 (Accelrys). The three other nonliganded human albumin structures in the PDB (ID codes 1BM0, 1E78, and 1UOR) overlay well with 1AO6 in the regions of interest, except for a small rotation of the side chain of His-247 in 1UOR. The model was imported into SYBYL V.6.8 (Tripos Associates, St. Louis) for energy minimization to optimize geometry, using the TRIPOS force field after some specific force-field parameters for zinc had been defined. Bond lengths for Zn^{2+} bound to histidine (2.00 Å), aspartate (2.00 Å), and water (2.06 Å) were taken from ref. 29, and the Zn^{2+}-O (Asn-99) distance (2.15 Å) was based on the published crystal structures of calcineurin and kidney bean purple acid phosphatase (PDB ID codes 1AUI, 1TCO, and 4KBP; refs. 30–32). Force constants were taken from the TRIPOS force field. Bond angles around zinc were not constrained. In a first step, the geometry around Zn^{2+} was optimized by 100 steps of energy minimization, taking into account only the Zn^{2+} ion, the four protein ligand residues, and the water molecule. A further 50 steps of energy minimization were then applied to residues 65–69, 97–101, 247–251, the Zn^{2+} ion, and the water mole-

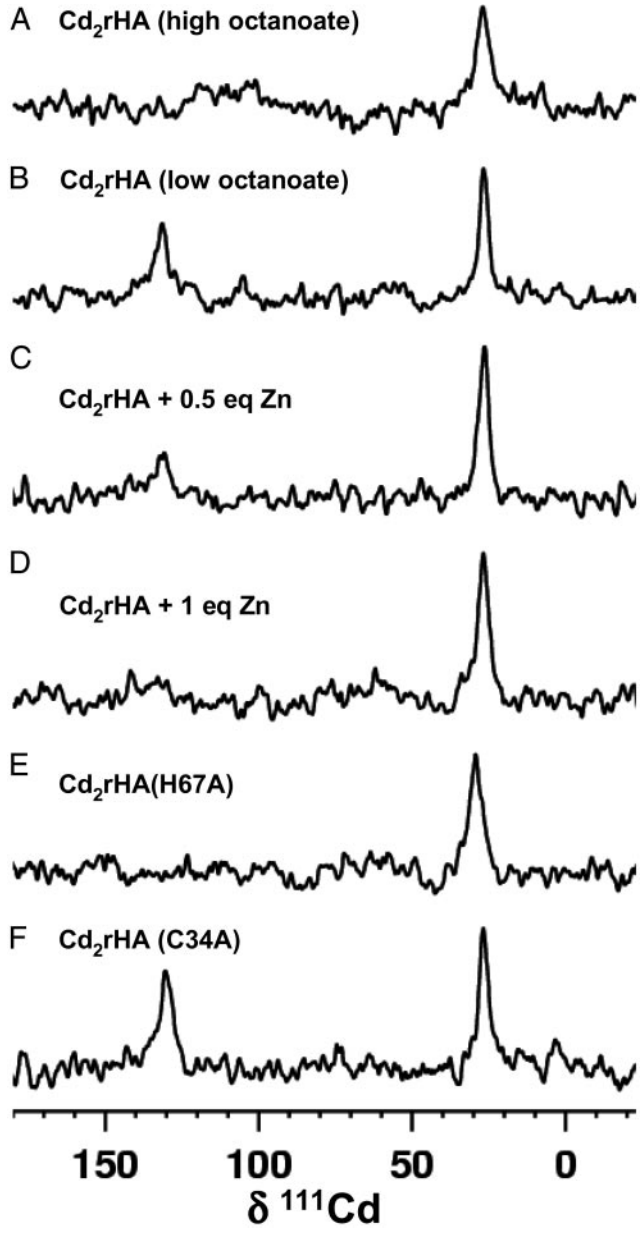

Fig. 2. ^{111}Cd-{^{1}H} NMR spectra of 1.5 mM rHA in the presence of 2 mol equivalent $^{111}CdCl_2$, pH 7.1/50 mM Tris·HCl/50 mM NaCl. (*A*) High octanoate (≈8 mol equivalent per mol of rHA). (*B*) Low octanoate (<4 mol equivalent octanoate per mol of rHA; obtained by dialysis of the rHA used in *A*). A similar sample prepared from charcoal-defatted rHA (33) gave an almost identical spectrum. (*C*) Low octanoate rHA plus 0.5 mol of equivalent $ZnCl_2$. (*D*) Low octanoate rHA plus 1 mol of equivalent $ZnCl_2$. (*E*) Low octanoate His67Ala mutant rHA. (*F*) Low octanoate Cys34Ala mutant rHA. ^{113}Cd NMR spectra similar to *B* have been reported for human albumin isolated from serum, for intact blood serum, and for bovine, equine, and canine serum albumins (18, 19, 24). The relative areas of the two peaks are close to 1:1.

cule to remove bad geometries and van der Waals contacts that had been introduced through atom movements in the first step. Finally, 30 more steps were applied to the entire protein for the same reason. The rms deviation between the original structure and the Zn^{2+} model is 0.15 Å for all atoms and 0.73 Å for the atoms of the ligand residues only.

Structure and Sequence Comparisons. The Swiss PDB VIEWER V.3.6 was used to analyze and overlay the 18 structures under consideration. Sequence alignments were carried out by using CLUSTALW (European Molecular Biology Laboratory-European Bioinformatics Institute).

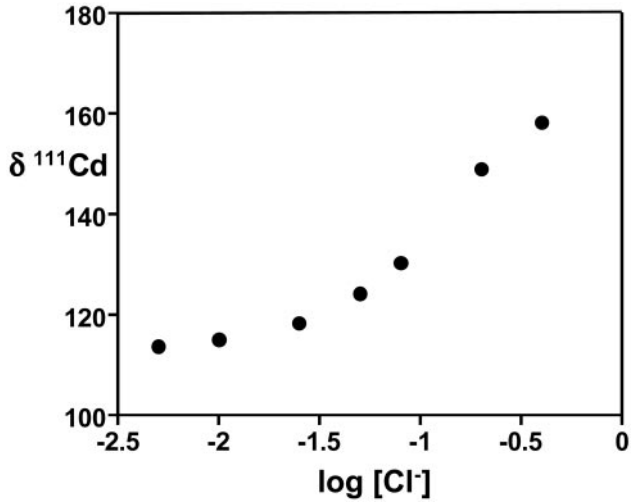

Fig. 3. Effect of chloride concentration on the ^{111}Cd NMR chemical shift of peak A of Cd_2-rHA. The binding is weak (fast exchange on the NMR time scale). From the curve, it is clear that the dissociation constant lies in the millimolar range. Peak B moves to low field by only 4.7 ppm over the same range of chloride concentrations.

Results and Discussion

Cd^{2+}-Binding Sites on Recombinant Human Albumin. Addition of $^{111}Cd^{2+}$ to 1.5 mM rHA (<4 mol equivalent bound octanoate) in 50 mM Tris·HCl containing 50 mM NaCl, pH 7.1, gave rise to ^{111}Cd NMR peaks at 131 (peak A) and 27 (peak B) ppm [relative to $Cd(ClO_4)_2$; Fig. 2*B*], indicative of Cd^{2+} sites containing 2–3 imidazole nitrogens and a single imidazole nitrogen, respectively, together with additional O ligands. Addition of 0.5 and 1 mol equivalent of $ZnCl_2$ to rHA in the presence of 2 mol equivalent of $^{111}Cd^{2+}$ resulted in a decrease in intensity of peak A (Fig. 2 *C* and *D*), suggesting that, for recombinant albumin as for serum albumins, site A has a greater affinity for Zn^{2+} than Cd^{2+}. In the reverse experiment (Fig. 6, which is published as supporting information on the PNAS web site), no ^{111}Cd peak for site A appeared when 2 mol equivalent of $^{111}Cd^{2+}$ was added to a solution of rHA containing 1 mol equivalent of $ZnCl_2$, confirming that Zn^{2+} binds more strongly to site A than Cd^{2+}.

The ^{111}Cd NMR spectrum of the mutant protein Cd_2-Cys34Ala-rHA contained the same 2 peaks A and B as native rHA (Fig. 2*F*), in agreement with data on BSA in which Cys-34 had been blocked by oxidation to a disulfide (24), thus confirming that Cys-34 is not involved in Cd^{2+} (and, therefore, probably not Zn^{2+}) binding. The thiol group of Cys-34 seems to have a low pK_a (<7; ref. 34), and examination of the x-ray structure of unliganded albumin suggests that its thiolate group may be stabilized by H-bonding to His-39 or Tyr-84; therefore, Cd^{2+} binding to the mutants His39Leu and Tyr84Phe was also studied. However, they too gave rise to the same ^{111}Cd NMR spectrum (Fig. 7, which is published as supporting information on the PNAS web site), suggesting that Cys-34 is not the locus for a strong Cd^{2+} site on rHA in either its deprotonated or protonated state.

Chloride Binds Weakly at Site A. Evidence that Cd^{2+} in site A can bind a nonprotein ligand was obtained from titrations of Cd_2-rHA with chloride ions. High chloride concentrations induced low-field shifts of peak A, but not peak B (Fig. 3). The magnitude of the overall shift (≈75 ppm) is similar to that observed

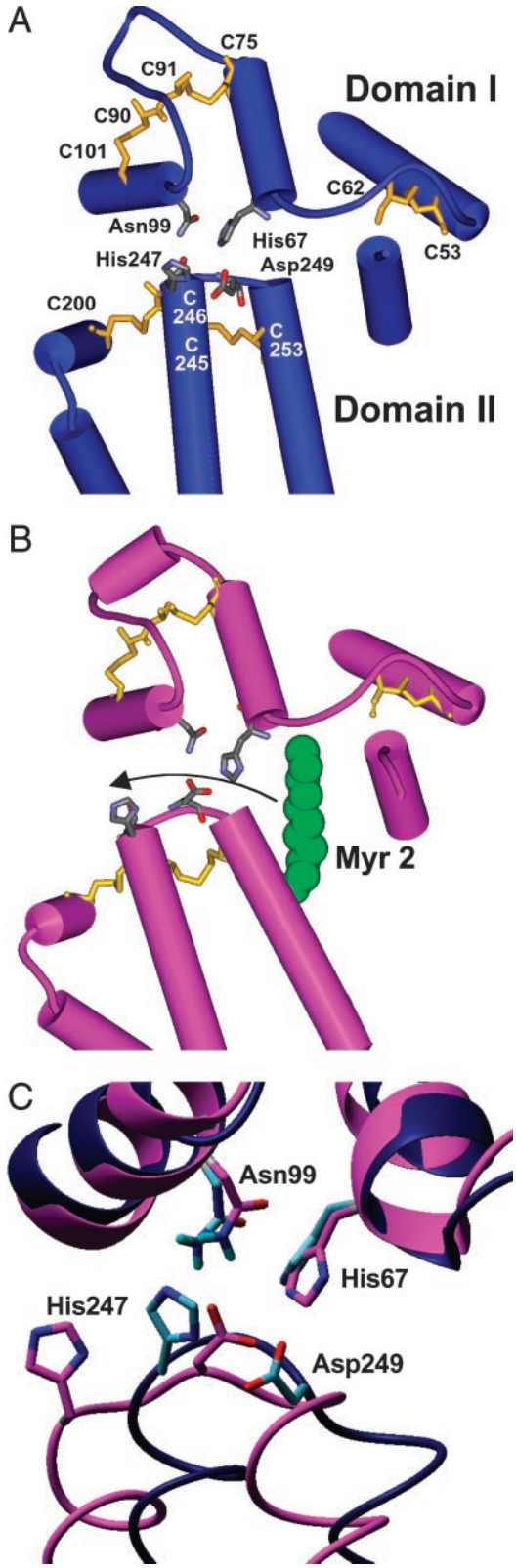

Fig. 4. Effect of fatty acid binding to site 2 on the proposed Zn^{2+}-binding site of human albumin. (*A*) Domain and secondary structure plus cystine-bridge network around the metal site in unliganded albumin (blue, PDB ID code 1AO6). The cystine residues (yellow) and the zinc ligands (CPK colors) are shown as stick models. (*B*) Domain and secondary structure of albumin with bound myristate (magenta, PDB ID code 1BJ5), with domain I in the same orientation as in *A*, showing the tilting of the two long helices in domain II induced by fatty acid binding in myristate site 2; myristate (green) is shown as a space-filling model. (*C*) The 4- to 6-Å movement of His-247 and Asp-249, which are situated in the loop connecting the two helices, away from His-67 and Asn-99. The overlay was generated in Swiss PDB VIEWER V.3.6 by aligning the backbone atoms of His-67 and Asn-99. The other 11 structures in the PDB of human albumin with bound fatty-acids (PDB ID codes: 1BKE, 5 myristates/2 triiodobenzoates; 1E7C, 5 myristates/7 halothanes; 1E7E, 10 caprates; 1E7F, 8 laurates; 1E7G, 8 myristates; 1E7H, 7 palmitates; 1E7I, 7 stearates; 1GNI, 7 oleates; 1GNJ, 8 arachidonates; 1H9Z, 6 myristates/1 R-warfarin; 1HA2, 6 myristates/1 S-warfarin) have similar shifts of His-247 and Asp-249. Other nonfatty acid-liganded structures [PDB ID codes: 1BM0, 1E78 (both unliganded), 1E7A (2 propofols), and 1E7B (3 halothanes)] have the four ligand residues arranged in as close proximity as 1AO6. In 1UOR, the backbone atoms of the four ligands are in approximately the same positions as in 1AO6, but the side chain of His-247 is rotated about the C(α)–C(β) bond such that the imidazole ring points away from the other three residues.

for Cl^--binding to aqua Cd^{2+} ions (35), and consistent with weak Cl^--binding at site A (binding constant estimated to be in the millimolar range). These findings explain why different chemical shifts have previously been observed for peak A from cadmium albumin in different media, including intact human blood serum [(Cl^-) = 95–105 mM].

Five-Coordinate Site at the Interface Between Domains I and II. Because all of the available evidence suggested that site A contains 2 or 3 N ligands, we searched for a region in the x-ray crystal structures of human albumin which brings two or three histidine side chains into close proximity for Zn^{2+}/Cd^{2+} coordination. We began our search with the four x-ray structures of albumin containing no bound fatty acids, of which PDB entry 1AO6 is typical. Only one such region (Fig. 1*A*) was identified. It involves His-67 and His-247, situated at the interface of domains I and II, and Asn-99 and Asp-249, candidates for providing two additional O ligands. Sequence comparisons showed that these four residues are completely conserved in all mammalian albumins sequenced to date (Fig. 8, which is published as supporting information on the PNAS web site).

The suitability of this region of the protein as a zinc-binding site was investigated by molecular modeling, employing a force-field-based energy minimization procedure. Even with the application of angle constraints, attempts to model a tetrahedral Zn^{2+}site involving only the four protein ligands yielded a distorted trigonal bipyramidal geometry with an empty equatorial binding site, suggesting the requirement for a fifth ligand. This requirement is consistent with the observed binding of chloride to Cd(A) (see above). An analysis of a database (36) for low molecular weight complexes revealed that the binding constants for Zn–Cl complexes are generally smaller by at least a factor of 10 than those of Cd–Cl complexes. Therefore, we estimate that at plasma chloride concentrations (95–105 mM), $<5\%$ of Zn(A) is likely to exist as a chloride complex, and that the fifth ligand *in vivo* may be water.

The resulting molecular model is shown in Fig. 1*B*. It is remarkable that only small movements of the four ligand residues are required to accommodate the Zn^{2+} ion; the rms deviation between starting structure (derived from 1AO6) and final model is only 0.73 Å for the atoms of the ligand residues. The proposed Zn^{2+} site has the two histidine nitrogens in the axial positions of a distorted trigonal bipyramid: His-67 coordinates to Zn^{2+} via Nε, and His-247 coordinates via Nδ. Other possible connectivities were tested but seemed to be less favorable. The nonprotein ligand, modeled as water, points toward the outside of the protein. Additional modeling attempts with different starting structures furnished sites with similar geometries. The close superposition of the modeled metal site and the starting structure strongly suggest that the site is "preformed" in the unliganded protein. The proposed zinc site lies at the

interface of domains I (His-67 and Asn-99) and II (His-247 and Asp-249). His-67 is situated at the N-terminal end of helix 4 and Asn-99 is at the N-terminal end of helix 6. The helices are connected by the C75-C91 and C90-C101 disulfide bridges (Fig. 4*A*). His-247 is at the C-terminal end of helix 13, and Asp-249 is situated in the loop connecting helices 13 and 14 in domain II. These helices are connected by the C245-C253 disulfide bridge, and a further disulfide bridge, C200-C246, mediates contact of these helices with other parts of the domain. In apo-albumin, the orientation of Asn-99 is constrained by H-bonding to Tyr-30 (Fig. 9*A*, which is published as supporting information on the PNAS web site), whereas Asp-249 is H-bonded to both His-67 and His-247.

Database searches revealed that the modeled site has the same set of amino acid ligands as Zn^{2+} in the enzymes human calcineurin, *E. coli* 5′-endonucleotidase and kidney bean purple acid phosphatase. However, for these enzymes, the Asp ligand bridges to a second metal ion (zinc or iron), and the fifth ligand (phosphate or carbonate) can form a second bridge between the metal ions. In all cases, the site is close to the surface of the protein (or domain), and the fifth coordination site is accessible to substrate or solvent. The geometries are distorted trigonal-bipyramidal or square-pyramidal, but whereas the N-Zn-N bond angle for albumin is 143°, this bond angle is closer to 90° in these enzymes.

Zn^{2+} in carboxypeptidase A also has two His, a carboxylate (bidentate Glu) and a water ligand, whereas the substrate (a peptide) coordinates via its amide oxygen (37). Hence, the intermediate in the enzymatic reaction has a similar set of Zn^{2+} ligands as the proposed Zn^{2+} site on albumin. It is notable that the Zn^{2+}-binding constants of albumin ($\log K_d = -7.53$) and carboxypeptidase A ($\log K_d = -7.3$; ref. 38) are very similar. Zn^{2+} in carboxypeptidase A also has a weak affinity for Cl^- ($\log K_d = -1.3$; ref. 39).

Mutation of His-67 Modifies Metal Binding. We synthesized a mutant in which one of the histidine ligands in the proposed zinc-binding site, His-67, is substituted by an amino acid with a nonbinding side chain, alanine. Addition of 2 mol equivalent of $^{111}Cd^{2+}$ to H67A-rHA gave rise only to ^{111}Cd peak B at 29 ppm (Fig. 2*E*). We also found that $^{111}Cd^{2+}$ addition to chicken serum albumin did not give rise to either peaks A or B. Chicken albumin contains His-67 → Pro (His67Pro) and His247Glu substitutions compared with human albumin, which would be expected to greatly reduce the affinity of Cd^{2+} for site A.

Fatty-Acid-Induced Switch at Metal-Binding Site A. It has been noted in published studies that the fatty acid content of serum albumin influences the appearance of ^{113}Cd peak A (24). We compared ^{111}Cd NMR spectra of Cd_2-rHA with high (≈8 mol/mol rHA) and low (<4 mol/mol rHA) octanoate content. Peak B was not affected by the variation in fatty acid loading, but peak A was not present in the high octanoate samples (Fig. 2*A*). We examined the 12 x-ray crystal structures of fatty-acid loaded albumin (see Fig. 4 caption) and found that the preorganization of site A is disrupted in all of them. This disruption arises from the binding of a fatty acid anion in so-called site 2 (14). Remarkably, this fatty acid-binding site is the only one identified in albumin crystals which is shared by two domains (14). The carboxylate end of the fatty acid interacts with Arg-257 and Ser-287 (both subdomain IIA), Tyr-150 (subdomain IB), and the methyl end with subdomain IA. To accommodate a fatty acid anion, the long helix connecting domains I and II bends, and the two half-sites in unliganded rHA move by more than 10 Å to form a continuous cavity (14). This fatty acid binding results in a movement of residues His-247 and Asp-249 (Fig. 4) by 4–6 Å away from the other two residues, His-67 and Asn-99, in the proposed Zn^{2+} site. Asp-249 also changes its side-chain conformation to maintain the H-bond to Nε of His-67 and forms an additional H-bond to Asn-99 (compare Figs. 8 *A* and *B*). His-247, which is H-bonded to Asn-99 in the unliganded structure, forms an H-bond with Glu-100 in the fatty acid-bound structures. The network of disulfide bonds (Fig. 5) partially rigidifies the frameworks on which the proposed Zn ligands are based and also provides a mechanism for interhelix communication of binding events in this region. It seems that fatty acid binding to site 2 triggers a spring-lock mechanism which disengages the upper (His-67/Asn-99) and lower (His-247/Asp-249) halves of the metal site.

Under normal physiological conditions, HSA carries one or two molecules of long-chain fatty acid (C_{16}-C_{20}; ref. 12), but up to eight binding sites have been identified (40). Two of the three high-affinity sites are thought to be located in domain III, and one is thought to be located in domain I. Fatty acid site 2 seems to be a low-affinity site which becomes populated only when fatty acid anions are highly abundant.

Conclusions

Previous work has shown that HSA has a strong binding site for Zn^{2+} (5) and plays a major role in the transport of this essential metal ion in blood and its delivery to cells and tissues (12). It has been proposed that the site involves at least two histidine ligands (23, 24), but no structural model of the site has been reported. Here, we have studied metal binding to recombinant human albumin, thus avoiding some of the problems associated with the heterogeneity of natural serum albumin (e.g., fatty acid and thiol content) encountered in previous reports.

Analysis of the x-ray structures of unliganded human albumin in the PDB led to the identification of only one potential metal site containing at least two His residues. It lies at the interface of domains I and II, and two additional potential ligands (Asp and Asn) are situated nearby, poised to form a five-coordinate site with a low molecular weight ligand such as water or Cl^- in the fifth coordination site. Weak Cl^--binding to Cd^{2+} in this site was detected for rHA.

The amino acids contributing to this site are highly conserved in mammalian albumins. The trigonal bipyramidal site is apparently "preformed" in unliganded albumin, although none of the reported x-ray structures seem to contain a metal ion bound here. Mutation of His-67 → Ala disrupted the binding of Cd^{2+}. Similar zinc sites are present in dinuclear phosphatases. Because the proposed albumin site is mononuclear, phosphatase activity is not expected, but the fifth coordination site could allow binding of a substrate or provide a low-energy pathway for transfer of zinc onto a suitable receptor.

Analysis of the available x-ray crystal structures of albumin and the ^{111}Cd NMR data presented here suggest that fatty acids disrupt metal binding to site A. This finding can be explained by the occupation of fatty acid site 2, which is thought to be a low-affinity site (14). This event triggers a movement of two of the proposed ligands (His-247 and Asp-249) by ≈5 Å away from His-67 and Asn-99, the two other proposed protein ligands in the Zn^{2+} site. It will now be of interest to explore the possible consequences of the interactive binding of Zn^{2+} and fatty acids to albumin. Crosstalk between Zn^{2+} and fatty acid status has already been proposed (41).

The proposed switching of the zinc site in human albumin by fatty acid binding is an intriguing example of an allosteric interaction between an organic nutrient and an essential metal ion. It might be possible to exploit this interaction in drug design and therapy.

We thank Dr. Chris Finnis (Delta Biotechnology Ltd.) for the production of the Cys34Ala rHA mutant, and Tony Greenfield and Lee Blackwell (Delta Biotechnology Ltd.) for help with expression and purification of mutant proteins. We also thank Dr. Sharon Kelly (University of Glasgow) for CD studies. We thank the Biotechnology and Biological Sciences Research Council and Delta Biotechnology Ltd. Council for Advancement and Support of Education award (to A.J.S.), the European Community Marie Curie Fellowship (to C.A.B.), and The Wellcome Trust (Edinburgh Protein Interaction Centre) for their support of this work.

1. Lipscomb, W. J. & Sträter, N. (1996) *Chem. Rev.* **96,** 2375–2433.
2. Klimpel, K. R., Arora, N. & Leppla, S. H. (1994) *Mol. Microbiol.* **13,** 1093–1100.
3. Håkansson, M., Antonsson, P., Björk, P. & Svensson, L. A. (2001) *J. Biol. Inorg. Chem.* **6,** 757–762.
4. Janc, J. W., Clark, J. M., Warne, R. L., Elrod, K. C., Katz, B. A. & Moore, W. R. (2000) *Biochemistry* **39,** 4792–4800.
5. Masuoka, J., Hegenauer, J., Van Dyke, B. R. & Saltman, P. (1993) *J. Biol. Chem.* **268,** 21533–21537.
6. Bobilya, D. J., Beiske-Anderson, M. & Reeves, P. G. (1993) *Proc. Soc. Exp. Biol. Med.* **202,** 159–166.
7. Tibaduiza, E. C. & Bobilya, D. J. (1996) *J. Cell. Physiol.* **167,** 539–547.
8. Gálvez, M., Moreno, J. A., Elósegui, L. M. & Escanero, J. F. (2001) *Biol. Trace Element Res.* **84,** 45–56.
9. Rabenstein, D. L. & Isab, A. A. (1980) *FEBS Lett.* **121,** 61–64.
10. Simons, J. J. (1991) *J. Membr. Biol.* **123,** 63–71.
11. Oelshlegel, F. R., Jr., Brewer, G. J., Knutsen, C., Prasad, A. S. & Schoomaker, E. B. (1974) *Arch. Biochem. Biophys.* **163,** 742–748.
12. Peters, T., Jr. (1995) *All About Albumin: Biochemistry, Genetics, and Medical Applications* (Academic, New York).
13. He, X. M. & Carter, D. C. (1992) *Nature* **358,** 209–215.
14. Curry, S., Mandelkow, H., Brick, P. & Franks, N. (1998) *Nat. Struct. Biol.* **5,** 827–835.
15. Sugio, S., Kashima, A., Mochizuki, S., Noda, N. & Kobayashi, K. (1999) *Protein Eng.* **12,** 439–446.
16. Bhattacharya, A. A., Curry, S. & Franks, N. P. (2000) *J. Biol. Chem.* **275,** 38731–38738.
17. Bal, W., Christodoulou, J., Sadler, P. J. & Tucker, A. (1998) *J. Inorg. Biochem.* **70,** 33–39.
18. Martins, E. O. & Drakenberg, T. (1982) *Inorg. Chim. Acta* **67,** 71–74.
19. Goumakos, W., Laussac, J. & Sarkar, B. (1991) *Biochem. Cell Biol.* **69,** 809–820.
20. Glennon, J. D. & Sarkar, B. (1982) *Biochem. J.* **203,** 15–23.
21. Laussac, J. P & Sarkar, B. (1984) *Biochemistry* **23,** 2832–2838.
22. Sadler, P. J., Tucker, A. & Viles, J. H. (1994) *Eur. J. Biochem.* **220,** 193–200.
23. Shaw, C. F., III (1989) *Comments Inorg. Chem.* **8,** 233–267.
24. Sadler, P. J. & Viles, J. H. (1996) *Inorg. Chem.* **35,** 4490–4496.
25. Sleep, D., Belfield, G. P., Ballance, D. J., Steven, J., Jones, S., Evans, L. R., Moir, P. D. & Croodey, A. R. (1991) *Biotechnology* **9,** 183–187.
26. Kerry-Williams, S. M., Gilbert, S. C., Evans, L. R. & Ballance, D. J. (1998) *Yeast* **14,** 161–169.
27. Sreerama, N. & Woody, R. W. (1994) *Biochemistry* **33,** 10022–10025.
28. Öz, G. L., Pountney, D. L. & Armitage, I. M. (1998) *Biochem. Cell Biol.* **76,** 223–234.
29. Harding, M. M. (2001) *Acta Crystallogr. D* **57**, 401–411, http://tanna.bch.ed.ac.uk.
30. Kissinger, C. R., Parge, H. E., Knighton, D. R., Lewis, C. T., Pelletier, L. A., Tempczyk, A., Kalish, V. J., Tucker, K. D., Showalter, R. E., Moomaw, E. W., *et al.* (1995) *Nature* **378,** 641–644.
31. Griffith, J. P., Kim, J. L., Kim, E. E., Sintchak, M. D., Thomson, J. A., Fitzgibbon, M. J., Fleming, M. A., Caron, P. R., Hsiao, K. & Navia, M. A. (1995) *Cell* **82,** 507–522.
32. Klabunde, T., Sträter, N., Fröhlich, R., Witzel, H. & Krebs, B. (1996) *J. Mol. Biol.* **259,** 737–748.
33. Chen, R. F. (1967) *J. Biol. Chem.* **242,** 173–181.
34. Pedersen, A. O. & Jacobsen, J. (1980) *Eur. J. Biochem.* **106,** 291–295.
35. Ackerman, J. J. H., Orr, T. V., Bartuska, V. J. & Maciel, G. E. (1979) *J. Am. Chem. Soc.* **101,** 341–347.
36. Pettit, G. & Pettit, L. D. (1993) *IUPAC Stability Constants Database* (IUPAC and Academic Software, Otley, U.K.).
37. Jensen, A. F., Bukrinsky, J. T., Bjerrum, M. J. & Larsen, S. (2002) *J. Biol. Inorg. Chem.* **7,** 490–499.
38. Rees, D. C., Lewis, M. & Lipscomb, W. N. (1983) *J. Mol. Biol.* **168,** 367–387.
39. Williams, A. C. & Auld, D. S. (1986) *Biochemistry* **25,** 94–100.
40. Petitpas, I., Grune, T., Bhattacharya, A. A. & Curry, S. (2001) *J. Mol. Biol.* **314,** 955–960.
41. Wauben, P. M., Xing, H.-C. & Wainwright, P. E. (1999) *J. Nutr.* **129,** 1773–1781.